JOURNAL OF VIROLOGY, Mar. 1996, p. 1890–1897 Vol. 70, No. 3
0022-538X/96/$04.00+0

RNA-Protein Interactions at the 3′ End of the Hepatitis A Virus RNA

YURI KUSOV,[1]* MANFRED WEITZ,[1] GÜNTER DOLLENMEIER,[1] VERENA GAUSS-MÜLLER,[2] AND GÜNTER SIEGL[1]

Institute of Clinical Microbiology and Immunology, CH-9000 St. Gallen, Switzerland,[1] and Institute of Medical Microbiology, Medical University of Lübeck, D-23586 Lübeck, Germany[2]

Received 22 August 1995/Accepted 11 December 1995

The regulative *cis*-acting terminal RNA structures and the proteins involved in the amplification of the hepatitis A virus (HAV) genome are unknown. By UV cross-linking/label transfer experiments, we have analyzed sequences of the 3′-nontranslated region (3′-NTR) and preceding domains of the viral genome for their ability to interact with host proteins. A series of cDNA constructs were used to create genomic- and antigenomic-sense transcripts. The results show that the 3′-NTR–poly(A) interacted with host cell proteins with molecular masses of 38, 45, 57, 84, and 110 kDa only weakly, compared with RNA structures also consisting of 3D-coding regions. Protein p38 was most efficiently labeled after interaction with secondary-structure elements located at the 3′ end of the HAV RNA. p38 also interacted with a 5′-terminal RNA probe. Optimal RNA binding was found to be dependent on the salt concentration. The specificity of the RNA-protein interaction was proven by competition assays. These data might indicate that a higher-order structure formed at the junction of the $3D^{pol}$-coding sequence and the 3′-NTR of the HAV genome (putative RNA pseudoknot) significantly improves binding of host proteins and thus suggests that this structure might be essential for the formation of the replication complex initiating minus-strand RNA synthesis.

The human hepatitis A virus (HAV) is a representative of the picornavirus family which differs significantly in its biological behavior from other members of the family (for a review, see reference 34). First, the virus has a unique tropism for liver cells in vivo. Second, because of their noncytolytic growth, most HAV strains do not shut down the host cells' macromolecular synthesis and the virus titer is relatively low in vitro compared with those of other picornaviruses. Third, HAV is distinct in utilizing only one virus-encoded protease for cleavage of the viral polyprotein (33). Because of these and other peculiarities, HAV was classified as the single member of a separate genus (*Hepatovirus*) of the *Picornaviridae* family (16). Nevertheless, there are features including the general genome organization that are shared with other picornaviruses (36). The plus-strand HAV RNA genome contains a single open reading frame encoding a large polyprotein of approximately 2270 amino acids which is cotranslationally processed, yielding mature structural and nonstructural proteins. The open reading frame is flanked by nontranslated regions (NTR) at both ends. Directly upstream of the open reading frame is located the internal ribosomal entry site (IRES), which is a *cis*-acting highly structured element which renders picornavirus translation cap independent. The structure and function of IRES have been intensively studied for poliovirus and encephalomyocarditis virus (EMCV) (25, 31; for a review, see reference 38). Instead of scanning from the 5′ end, the 40S ribosomal subunit directly binds to this internal region of the 5′ NTR, which is located between nucleotides (nt) 151 and 735 of the HAV genome (8).

In addition to its messenger function, the viral RNA of picornaviruses has to serve in a second, possibly competing process which proceeds in the direction opposite to translation. Starting at the 3′ end of the genome, the viral RNA acts as a template for the virus-encoded polymerase $3D^{pol}$ to yield minus strands from which in turn new plus strands are synthesized (for reviews, see references 30 and 38). For the most distal regions of either RNA terminus, higher-order structures have been proposed which are essential as recognition signals for the viral polymerase (2, 3, 12, 21, 28). This enzyme was shown to exclusively replicate viral RNA in vivo (15). Multiple models have been proposed for the plus-strand synthesis of poliovirus which takes place in the membrane-associated replication complex (2, 18, 20). Genetic and biochemical evidence supports the idea that viral as well as host cell proteins are implicated in viral RNA synthesis (18, 24). In particular, the cloverleaf structure at the 5′ end of poliovirus RNA is required for efficient binding of the viral proteinase $3CD^{pro}$, $3AB^{primer}$, and several host cell proteins, including p36, which was identified as the N-terminal fragment of EF-1a (2, 3, 20).

The 3′-NTR of picornavirus RNAs is shorter than the 5′-NTR and contains a poly(A) tract at the end (21). It can form secondary- and tertiary-structure elements, consisting of stem-loops and involving the poly(A) tail in base pairing (14, 28). The propensity to form a pseudoknot (PK) or possibly a tRNA-like structure has been described for the 3′-terminal RNA sequence of poliovirus and coxsackievirus B1 (20, 21, 28). Although recognition of the 3′ end of the viral RNA by the viral polymerase must be one of the first steps in RNA amplification, the functional role of the 3′ terminal region and *cis*-acting recognition signals therein have not been studied in detail, and host proteins implicated in minus-strand RNA synthesis are unidentified. Very recently, direct evidence that $3CD^{pro}$ of poliovirus not only binds to the 5′ cloverleaf but is also cross-linked to 3′-terminal sequences in the presence of viral protein 3AB has been reported (20). In contrast, $3D^{pol}$ of EMCV specifically interacts with the 3′-NTR–poly(A) fragment of EMCV RNA (12).

To understand the replicative features of HAV which result in unusually slow growth and to extend our initial studies using persistently infected cells (26), we here assessed the function of the 3′-terminal HAV RNA sequence by studying its properties of binding to host cell proteins. Using UV cross-linking/label

* Corresponding author. Present address: Institute of Medical Molecular Biology, Medical University of Lübeck, Ratzeburger Allee 160, D-23538 Lübeck, Germany. Phone: 49 451 500 4085. Fax: 49 451 500 3637. Electronic mail address: koussov@molbio.mu-luebeck.de

transfer assays, we show here that host proteins, in particular p38, p45, p57, and p84, specifically interact not only with the 3′-NTR of the HAV genome but also with sequences preceding the 3′-NTR and extending into the $3D^{pol}$-coding region. Interestingly, protein p38 was shown to interact also with the RNA sequences of the 5′-NTR and might be identical to a previously described IRES-binding protein (10).

MATERIALS AND METHODS

Virus strains and cells. HAV strains CLF, HAS-15, and HM175/18f were used to infect MRC-5 (human diploid lung fibroblast), FRhK-4 (fetal rhesus monkey kidney), and BS-C-1 (continuous African green monkey kidney) cells, respectively. The multiplicity of infection was usually 10 50% tissue culture infective doses ($TCID_{50}$) per cell. The conditions of maintaining mock- and HAV-infected cells and of determination of viral antigen expression were similar to those described before (13). The CLF and HAS-15 strains reached the maximum infectious titer (approximately 10^7 to $10^{7.5}$ $TCID_{50}$ per ml) at 14 to 21 days postinfection, while strain HM175/18f reached a titer of 10^8 $TCID_{50}$ per ml at 8 to 10 days postinfection.

Preparation of cell extracts. At the same time postinfection, S-100 cell extracts were prepared from mock- and HAV-infected cells by the procedure described by Chang et al. (10). Briefly, mock- or HAV-infected cells were removed from monolayers mechanically, collected by centrifugation at 150 to 200 × *g* for 20 min at 4°C, and washed twice with phosphate-buffered saline. The cells were carefully resuspended in approximately 4 packed-cell volumes of hypotonic buffer containing 10 mM *N*-2-hydroxyethylpiperazine-*N*′-2-ethanesulfonic acid (HEPES; pH 7.0), 10 mM KCl, 1.5 mM $MgCl_2$, 0.5 mM dithiothreitol (DTT), and phenylmethylsulfonyl fluoride. After homogenization of the cell suspension by 50 to 60 strokes with a Dounce homogenizer, the nuclei were removed by centrifugation at 4,300 × *g* for 10 min at 4°C and the resulting supernatant was centrifuged at 100,000 × *g* for 1 h at 4°C. The supernatant was stored in aliquots at −70°C after adjustment to buffer A conditions (20 mM HEPES [pH 7.9], 100 mM KCl, 1.1 mM $MgCl_2$, 0.37 mM DTT, 0.2 mM EDTA, 0.2 mM phenylmethylsulfonyl fluoride, 20% glycerol). Extracts of cytoplasmic proteins were similarly prepared from mock-infected buffalo green monkey (BGM) cells, continuous monkey kidney (Vero) cells, HeLaS3 cells, and the T7 RNA polymerase-expressing derivative of BS-C-1 cells (BT7-H) (37). The ribosome-associated proteins were prepared according to the following procedure. The 100,000 × *g* pellet was resuspended in an ice-cold buffer containing 0.25 M sucrose, 1 mM DTT, and 0.1 mM EDTA (pH 7.0). A 4 M concentration of KCl was slowly added to the ribosome suspension to give a final concentration of 0.5 M. After incubation on ice for 1 h and removal of the ribosomes by centrifugation at 100,000 × *g* for 2 h at 4°C, the supernatant was dialyzed overnight against buffer A and stored in aliquots at −70°C (ribosomal salt wash [RSW]).

Construction of plasmids. DNA manipulation and cloning were performed in accordance with standard methods (32). The 3′-terminal HAV sequences were inserted into vector pGEM-1 (Promega) under the control of the SP6 and T7 promoters. To obtain a cDNA construct covering exclusively the 3′-NTR of HAV RNA, plasmid pHAV/7 (11) bearing the complete HAV genome of strain HM175 was restricted with *Bsp*HI, filled in with Klenow polymerase, and then restricted with *Eco*RI. The gel-isolated 90-nt fragment (nt 7410 to 7499) was ligated into pGEM-1, which had been previously opened with *Hin*cII and *Eco*RI. From this construct, RNA90 was derived. A longer HAV cDNA fragment, containing 502 bases of the 3′ end, was excised from pHAV/7 with *Xho*I and *Eco*RI and after gel purification was reinserted into pGEM-1, which had been previously cut with *Sal*I and *Eco*RI. The resulting plasmid gave rise to RNA502, and after linearization with *Bsp*HI, RNA413 was obtained. Finally, a 1,583-nt fragment encoding the complete $3D^{pol}$ and ending also with the poly(A) tract was excised from pHAV/7 with *Ssp*I and *Eco*RI, was gel purified, and was reinserted into pGEM-1 that had been cut with *Hin*cII and *Eco*RI. This construct was the source of RNA1583. The 5′-terminal RNA354 (first 354 nt of the HAV genome) was prepared by runoff transcription of plasmid pHAV/7, which had been linearized with *Hpa*I. The nucleotide sequences of all new plasmids were confirmed by dideoxy sequencing with appropriate primers and the DNA sequencing kit of U.S. Biochemicals (Sequenase 2).

RNA transcription and polyribonucleotides. To generate positive- or negative-sense HAV 3′-terminal radioactive RNA probes by runoff transcription, purified plasmid DNAs were linearized within the multiple cloning site of the vector by restriction with *Xba*I or *Hin*dIII and were transcribed with SP6 or T7 RNA polymerase, respectively (MAXIscript SP6/T7; Ambion), with [α-^{32}P]UTP (3,000 Ci/mmol) or [α-^{33}P]UTP (2,000 Ci/mmol; NEN) as described by the manufacturer. The radioactive RNAs were digested with RNase-free DNase at 37°C for 30 min and were electrophoresed through a nondenaturing 5% polyacrylamide gel. Full-length transcripts visualized by autoradiography were eluted by submerging the gel slice overnight at 4°C in a buffer containing 0.5 M ammonium acetate, 1 mM EDTA, and 0.1% sodium dodecyl sulfate (SDS). Unlabeled RNAs used in competition experiments were prepared in a similar way. The quality of transcripts was analyzed by formaldehyde gel electrophoresis. To assess the influence of vector-derived sequences on RNA-protein interaction, control RNA probes were transcribed from pGEM-1 by using SP6 or T7 RNA polymerase. After linearization with either *Xba*I or *Hin*dIII, transcripts of 28 (control RNA-pos) or 58 (control RNAneg) nt, respectively, were prepared by the procedure described above. To receive control RNA probes comparable in size to HAV-specific probes, plasmid pΔ355 (a kind gift of S. Lemon) was linearized with *Nsi*I, which was followed by transcription with SP6 RNA polymerase. The resulting transcript (control RNA178) represents HAV RNA sequence from nt 355 to 532 (178 nt) of the 5′-NTR. A longer control RNA probe was transcribed with T7 RNA polymerase from plasmid pET15b-2B which had been previously linearized with *Blp*I. The resulting transcript (control RNA753) represented the internal HAV sequence encoding HAV protein 2B (nt 3238 to 3990).

Poly(A), poly(U), poly(I,C), poly(T), and oligo(dT) were purchased from Sigma. tRNA from *Escherichia coli* MRE-600 (RNase-free) was obtained from Boehringer Mannheim.

The secondary-structure prediction. To evaluate the secondary structures of HAV RNAs, the RNAFOLD program described by Jaeger et al. (22), which is included in the Genetics Computer Group sequence analysis software package for the VAX, was employed. Folding energies used in this program were defined by Freier et al. (17). The PK structure at the 3′ end of the HAV genome was predicted in analogy to the previously described element of coxsackievirus B1 (21).

UV cross-linking. UV cross-linking of RNA-protein complexes was performed as described by Chang et al. (10). Briefly, cell extract (2 to 5 μg of protein) was incubated for 20 min at 30°C with the radioactive RNA probe (0.5×10^6 to 2×10^6 cpm) in binding buffer (5 mM HEPES [pH 7.9], 25 mM KCl, 2 mM $MgCl_2$, 1.75 mM ATP, 6 mM DTT, 0.05 mM phenylmethylsulfonyl fluoride, 0.05 mM EDTA, 5% glycerol) containing 30 μg of tRNA (when indicated) in a total volume of 60 μl. In competition experiments, the standard binding reaction was performed with unlabeled RNA in an approximately 50-fold molar excess before the radioactive RNA probe was added, and incubation continued at 30°C for further 20 min. The binding mixture was transferred to a 96-well plate and irradiated on ice at a distance of 2 to 4 cm for 60 min at 254 nm with a UV light source (Stratalinker 1800). After irradiation, RNA was digested with 20 μg of RNase A and 20 U of RNase T_1 at 37°C for 30 min. The products of cross-linking reactions were analyzed by SDS-12% polyacrylamide gel electrophoresis (PAGE). The gel was fixed, dried, and autoradiographed. Signal intensity was quantitated with an OPTOQUANT (Computer & Vision, Lübeck, Germany) and was expressed as mean values of two independent experiments. The intensity of the p38 band labeled by radioactive RNA502, as well as the extent of competition produced by unlabeled RNA502, was considered to correspond to 100 relative units.

RESULTS

RNA transcripts of the 3′ end of the HAV genome fold into different secondary structures. To assess the role of the 3′-terminal segments of the HAV RNA in interaction with cytoplasmic and ribosomal proteins of mock- and HAV-infected cells, a variety of RNA probes covering different parts of the 3′ end of the HAV genome were prepared (Fig. 1A). Whereas RNA90 represents the complete 3′-NTR which is followed by poly(A), RNA413 contains the sequence which precedes the 3′-NTR and encodes the C-terminal domain of polymerase $3D^{pol}$. In addition to the $3D^{pol}$-coding sequence, RNA502 consists of the 3′-NTR and the poly(A) tract. The complete $3D^{pol}$-coding region in addition to the 3′-NTR–poly(A) is present within RNA1583. With these RNA probes, the role of secondary-structure elements (stem-loops, cloverleaf-like elements, and/or PK) in RNA-protein interaction was evaluated. To illustrate the most important secondary-structure elements located at the 3′ end of the HAV RNA, the computer-predicted folding of the sequence downstream of nt 7363 is depicted in Fig. 1B. In addition to three stem-loops, a PK involving the base pairing of nt 7367 to 7373 and nt 7427 to 7433 can be resumed by RNA502 and RNA1583, both of which contain 3′ terminal coding and noncoding sequences. RNA90, which consists of sequences downstream of nt 7410, can form only stem-loops 7420 to 7455 and 7456 to 7481, whereas RNA413 extending to nt 7410 contains stem-loop 7383 to 7410, which is shown in Fig. 1B. Although some noncanonical base pairs could not be formed by the 5′ terminal sequence of the negative-sense HAV RNA, it still folded into a similar secondary structure (data not shown). Several additional stem-loops were created by computer folding within the 3D-coding sequence,

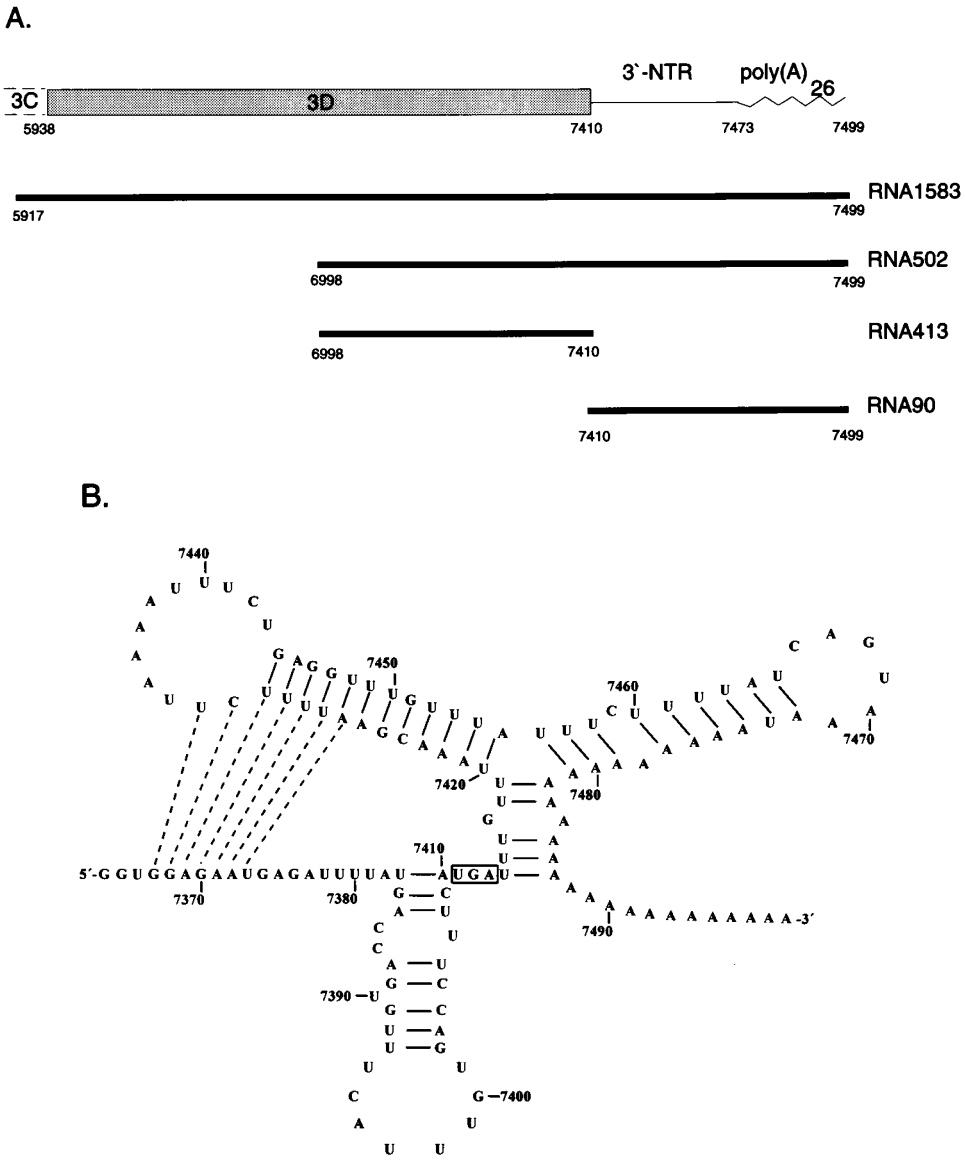

FIG. 1. (A) Schematic diagram of RNA probes representing the 3′-terminal region of HAV RNA, with the poly(A)$_{26}$ tract included. Plus-strand (coding) and minus-strand transcripts were created with either SP6 or T7 RNA polymerase. (B) Proposed stem-loop and PK structures at the 3′ terminus of the HAV genome. The nucleotide numbering is taken from that used for HAV strain HM175 (14); the translational termination codon is boxed. Dashed lines, alternative base pairing (PK structure).

preceding the PK element, in RNA413 as well as in RNA1583 (data not shown). All HAV RNA probes included a few additional bases derived from vector sequences. To exclude their impact on HAV-specific RNA-protein interaction, a series of control RNA probes were prepared by runoff transcription of pGEM-1 (control RNApos and control RNAneg). Control RNA probes comparable in size to HAV-specific RNAs were also prepared by runoff transcription within the HAV 5′-NTR (control RNA178) and 2B-coding sequence (control RNA753).

3′-terminal HAV RNA interacts with proteins present in the S-100 extract and RSW of mock- and HAV-infected cells. The interaction of RNA with proteins present in S-100 extract and RSW was determined by UV cross-linking/label transfer assays with RNA502. Extracts of mock- and HAV-infected MRC-5 cells harvested on the same day postinfection were prepared as described in Materials and Methods. RNA502 of genomic (RNA502pos) and antigenomic (RNA502neg) polarity was uniformly labeled with [α-^{32}P]UTP or [α-^{33}P]UTP and was incubated in binding buffer with cell extracts (S-100 or RSW). Subsequently, the mixture was exposed to a UV light source and digested with RNase A and RNase T_1 prior to separation by SDS-PAGE. A similar reaction was performed with the control RNA probes derived from pGEM-1, part of the IRES or 2B-coding sequences. The appearance of radioactively labeled proteins and the intensity of the bands served as a measure for RNA-protein binding.

The data presented in Fig. 2 demonstrate that various proteins present in the S-100 extracts and RSW of mock- and HAV-infected MRC-5 cells showed a capacity for specific binding to HAV RNA502. Cytoplasmic proteins with apparent molecular masses of approximately 38, 45, 57, 84, and 110 kDa were labeled with RNA502 of either polarity (Fig. 2A and B,

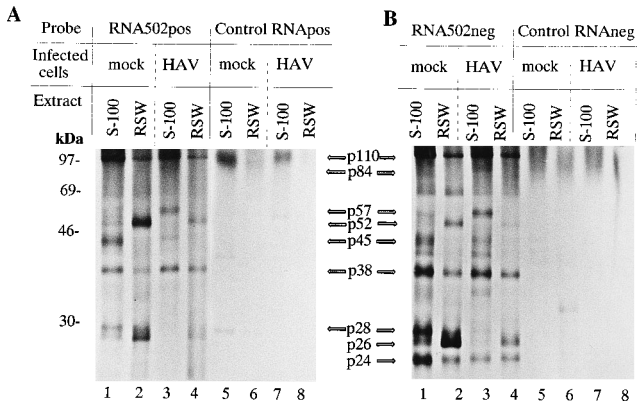

FIG. 2. Label transfer to RSW and cytoplasmic (S-100) proteins present in mock- and HAV-infected MRC-5 cells harvested 23 days after infection. After UV cross-linking to genomic-sense RNA502pos (A [lanes 1 to 4]) and antigenomic-sense RNA502neg (B [lanes 1 to 4]) and digestion with nucleases, the reaction mixture was analyzed by SDS-PAGE. Comparison with control RNAs transcribed from pGEM-1 by SP6 (A [lanes 5 to 8]) or T7 RNA polymerase (B [lanes 5 to 8]) is shown. The mobilities of radioactive marker proteins are given on the left; the positions of UV cross-linked proteins are marked by arrows.

lanes 1 and 3). Whereas p57 was found predominantly in S-100 of infected cells, proteins p28 and p26 were mainly demonstrable in S-100 extracts of mock-infected cells. In contrast, protein p45 was detected in mock- as well as in HAV-infected cells (compare lanes 1 and 3). Protein p38 found in mock- as well as in HAV-infected cells was common to all cells tested thus far (see below). Probably because of its greater stability during storage and/or freeze-thawing, protein p38 was more intensively labeled in later experiments than other proteins. In contrast to S-100 extracts, the spectra of ribosomal proteins in RSW were almost identical in mock- and HAV-infected cells, although protein p52 in RSW of mock-infected cells was labeled to a larger extent (Fig. 2, lanes 2 and 4). The main difference between genomic- and antigenomic RNA502 was detected among the low-molecular-weight proteins (p24, p26, and p28), which were significantly more reactive with the antigenomic probe (Fig. 2B, lanes 1 to 4). The protein with a molecular mass of approximately 110 kDa bound unspecifically to RNA, since its reactivity was partially inhibited by the addition of tRNA (see below).

Although they were used in a higher molar ratio (the same amounts of radioactivity were used for all cross-linking/label transfer mixtures, irrespective of the RNA size), control runoff transcripts of pGEM-1 were unable to transfer label to the proteins (Fig. 2, lanes 5 to 8). The protein detected as a faint band in the S-100 extract of HAV-infected cells with control RNApos (Fig. 2A, lane 7) had a slightly higher molecular mass than p57, which was labeled by RNA502pos (lane 3). As shown below (see Fig. 4), longer control RNA probes were also not able to transfer the label to any of the host proteins. Taken together, the results indicate that RNA representing the last 502 nt of the HAV genome specifically binds to cytoplasmic and ribosomal host cell proteins. Obviously, the positive- and negative-sense transcripts seem to fold into similar higher-order structures, resulting in comparable binding patterns (see also reference 20). Among the cytoplasmic proteins present in HAV-infected cells, an additional 57-kDa protein was detected.

RNA-binding efficiency varies under different ionic conditions. The binding of nucleic acids to proteins is known to be sensitive to the salt concentration (7, 10). The optimal binding condition for the interaction of host proteins with 3′ terminal sequences was determined by using increasing potassium concentrations. RNA502 was used as a source of radioactivity to transfer the label to cytoplasmic proteins present in HAV-infected MRC-5 cells. In this and the following experiments, relatively more label was transferred to p38 than that shown in Fig. 2. Because of the presence of high salt concentration in the S-100 extract (100 mM), only minimal amounts of potassium chloride were added to the binding mixture. By comparing the intensities of p38 bands at different potassium chloride concentrations (Fig. 3), it was obvious that the efficiency of transfer of label to p38 strongly decreased with increasing potassium concentrations. The situation was similar for p84, although the radioactive signal was much less intensive than that for p38. Whereas the intensities of p57 remained almost equal at all potassium concentrations tested, increasing concentrations of potassium enhanced the efficiency of transfer of label to some high-molecular-mass proteins (e.g., 110 kDa). Thus, binding of the cytoplasmic proteins p38 and p84 to RNA502 was optimal at a low potassium concentration, whereas that of p57 was independent of the amount of salt.

To test whether other cells contain p38, UV cross-linking/label transfer studies were carried out with S-100 extracts prepared from some mammalian cells. p38 was found in various HAV-susceptible cells tested so far (e.g., MRC-5, BS-C-1, and its derivative BT7-H, HeLaS3, Vero, BGM, and FRhK-4 [data not shown]).

^{33}P-labeled RNA probes representing different domains of the 3′-terminal HAV genome transfer the label to cytoplasmic proteins to various extents. To investigate the effects of RNA size and secondary structure on the binding specificities of p38 and p57, the cross-linking efficiencies of the 3′-terminal RNA transcripts depicted in Fig. 1A were determined. RNA probes

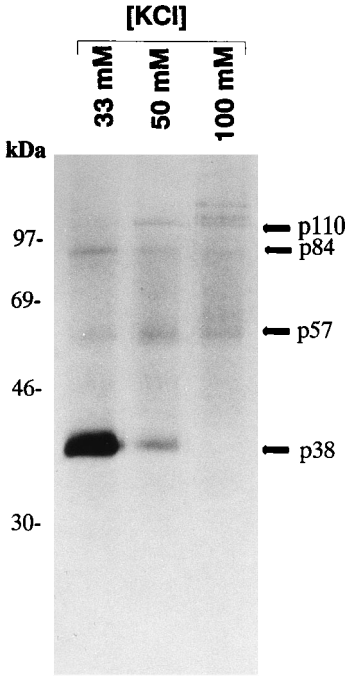

FIG. 3. Transfer of label to cytoplasmic proteins present in the S-100 extract of HAV-infected MRC-5 cells after UV cross-linking to genomic RNA502 under conditions of increasing potassium chloride concentrations. The mobilities of marker proteins and the positions of cross-linked proteins are shown on the left and right sides, respectively.

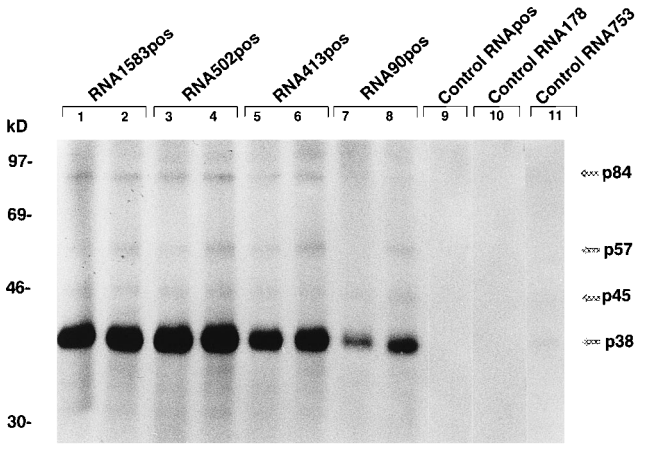

FIG. 4. Transfer of label to proteins present in S-100 extracts of mock (lanes 1, 3, 5, and 7)- and HAV (lanes 2, 4, 6, and 8 through 11)-infected MRC-5 cells after UV cross-linking to transcripts representing different segments of the 3′-terminal genomic-sense HAV RNA. The molecular masses of marker proteins are indicated on the left. The mobilities of cross-linked proteins of interest are marked by arrows.

consisting of vector-transcribed sequence (control RNApos) or transcribed either from a part of the IRES element of HAV RNA (control RNA178) or from internal RNA sequence coding for HAV 2B (control RNA753) were used as controls.

The data presented in Fig. 4 demonstrate that all 3′ terminal RNA probes were able to transfer the label to p38, p45, p57, and p84, which are present in the S-100 extract of mock (lanes 1, 3, 5, and 7)- and HAV (lanes 2, 4, 6, and 8 through 11)-infected MRC-5 cells. Control RNApos and RNA178 were unable to transfer the label to host protein(s) present in HAV-infected cells (lanes 9 and 10, respectively), while the transfer from control RNA753 was at the background level (lane 11). Compared with the results shown in Fig. 2, relatively more label was transferred to p38, which was confirmed by other experiments. Thus, p38 was considered the main RNA-binding protein. p57 was detected in higher abundance in HAV-infected cells than in mock-infected cells. Although equal amounts of radioactivity (thus, higher concentrations of the shorter RNAs with lengths of 90 and 413 nt) were used, more label was transferred to p38 by ^{33}P-labeled RNA502 and RNA1583 than by RNA413 and, in particular, by RNA90. The efficiencies of the label transfer from different RNA probes to p38 were quantitatively compared by scanning the intensity of the p38 band (the data are mean values of two independent experiments). The intensity of p38 cross-linked to radioactive RNA502 was considered 100 U. The sum of the intensities of p38 produced by RNA413 (53.2 U) and RNA90 (14.7 U) was less than that of RNA502 (100 U), thus indicating that structural elements required for efficient protein binding are not present in either RNA413 or RNA90 but are contained within RNA502 and RNA1583 (see below). The slightly decreased reactivity of RNA1583 (76.6 U) compared with RNA502 can be explained by the three times-lower molar ratio of this RNA probe which was used for the UV cross-linking/label transfer experiment. The data regarding the reactivities of various radioactive RNA probes correlate with the ability of unlabeled RNAs to compete for transfer of label to p38 (see below). In accordance with the results presented above, the antigenomic transcripts transferred the label additionally to a low-molecular-weight protein (p26) which was found predominantly in mock-infected cells (data not shown). These results indicate that RNA transcripts consisting of both the 3′-NTR–poly(A) and parts of the 3D^{pol}-coding region bind cytoplasmic proteins more efficiently than RNA containing only either segment. A similar pattern of cross-linked proteins was obtained for mock- and HAV-infected BS-C-1 and FRhK-4 cells, respectively (data not shown).

Enhanced interaction of 3′-terminal HAV RNAs requires a putative PK structure. To ascertain that binding of cytoplasmic proteins to the 3′-terminal RNA fragments of the HAV genome is specific and optimal when a higher-order structure is formed between sequences of the coding and noncoding regions, series of competition experiments were performed with an approximately 50-fold molar excess of unlabeled HAV transcripts of genomic or antigenomic sense. The extent of inhibition of label transfer was evaluated by measuring the intensity of the p38 band; the inhibition caused by unlabeled RNA502 was considered 100 relative U. The data presented in Fig. 5A demonstrate that RNA1583, consisting of the sequence encoding all of 3D^{pol} and the 3′-NTR–poly(A) fragment, efficiently competed (106 U) with radioactive RNA502 for label transfer to proteins p38, p57, p84, and p110, which are present in the S-100 extract of HAV-infected MRC-5 cells (lane 2). The competition for the label transfer caused by unlabeled RNA413, which encodes the C terminus of 3D^{pol}, as well as RNA90, which contains only the 3′-NTR–poly(A) fragment, was less pronounced (93 and 15 U [lanes 4 and 5, respectively]). The control transcript derived from pGEM-1 did not compete with radioactive RNA502 (1 relative U [lane 6]), thus confirming the specificity of competition caused by the HAV RNAs. Competition of unlabeled antisense RNA1583neg (98 relative U [Fig. 5B, lane 2]), RNA502neg (100 U [lane 3]), and RNA90neg (19 U [lane 4]) for binding with radioactive RNA502 of negative polarity suggests that sense and antisense transcripts resume a similar configuration. The lack of competition caused by control RNAneg confirmed the specificity of RNA-protein interaction (2 U [lane 5]).

Similar results were obtained when interaction of antigenomic RNA90neg and RNA1583neg with proteins present in the S-100 extract of HAV-infected MRC-5 cells was inhibited with other transcripts of negative polarity. The data presented in Fig. 6 clearly indicate that label transfer from both RNA90neg and RNA1583neg to protein p38 could be efficiently inhibited by an approximately 50-fold molar excess of

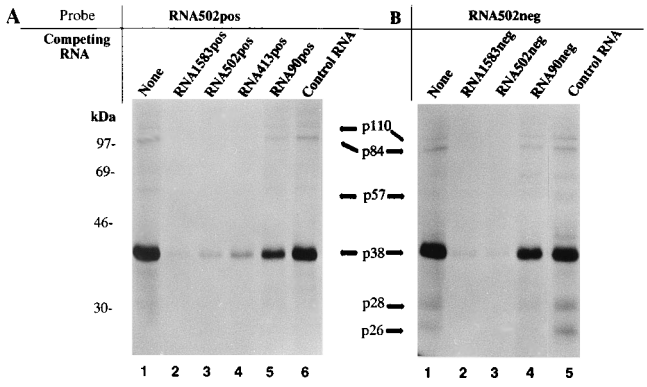

FIG. 5. Competition experiments to demonstrate the various specificities of binding of 3′-terminal RNA transcripts to cytoplasmic proteins of HAV-infected cells. Binding of RNA502 of positive (A) and negative (B) polarity was inhibited with unlabeled transcripts of the same polarity used in an approximately 50-fold molar excess. In lanes 1, water instead of unlabeled RNA was included in the reaction mixtures. The molecular masses of marker proteins are indicated on the left. The mobilities of cross-linked proteins of interest are marked by arrows.

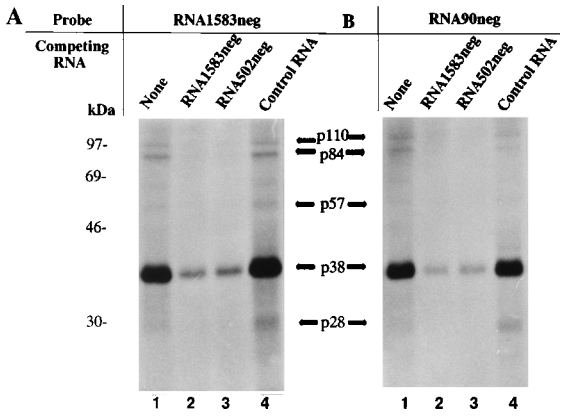

FIG. 6. Competition between labeled anti-genomic-sense RNA1583neg (A) and RNA90neg (B) with unlabeled RNA1583neg (lanes 2), RNA502neg (lanes 3), and control RNAs (lanes 4) for the transfer of label to proteins present in S-100 extracts of HAV-infected MRC-5 cells. In lanes 1, water instead of unlabeled RNAs was included in the reaction mixtures.

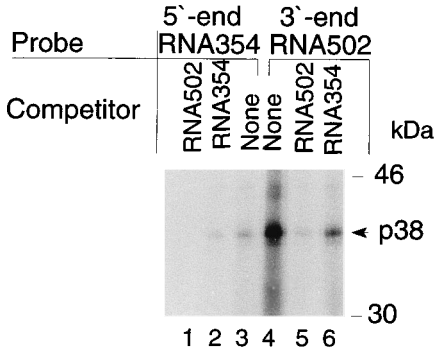

FIG. 8. Transfer of label to p38 present in the S-100 extract of BS-C-1 cells from 5′-terminal RNA354 (lane 3) and 3′-terminal RNA502 (lane 4) and competition data. A 50-fold molar excess of indicated competitor (lanes 1, 2, 5, and 6) was added to the binding mixture prior to the addition of the radioactive RNA probe. The molecular size standards and protein p38 are shown.

unlabeled RNA1583 (lanes 2) and RNA502 (lanes 3), thus suggesting the crucial role of higher-order structure elements formed by coding and noncoding regions. The unlabeled control (vector-transcribed) RNA did not compete with radioactive RNA transcripts for the label transfer to p38 (lane 4), demonstrating the specificity of the RNA-protein interaction.

Taken together, the competition data suggest that RNA structures formed not only by all or parts of the 3D-coding region but also by the 3′-NTR are essential for binding to proteins in HAV-infected cells. In accordance with the above-mentioned data, radioactive RNA90pos, representing 3′-NTR–poly(A), not only weakly interacted with p38 (Fig. 4) but also could not compete with RNA502 as efficiently as other RNAs for label transfer to p38 (Fig. 5).

To assess the role of the poly(A) tail for the interaction of the 3′-NTR with cytoplasmic proteins, competition experiments with homo- and heteropolymeric deoxyribo- and ribonucleotides were performed (Fig. 7). As expected, poly(U) (lane 5), poly(I,U) (lane 6), poly(T) (lane 8), and oligo(dT) (lane 9) inhibited binding to genome-sense RNA502, probably

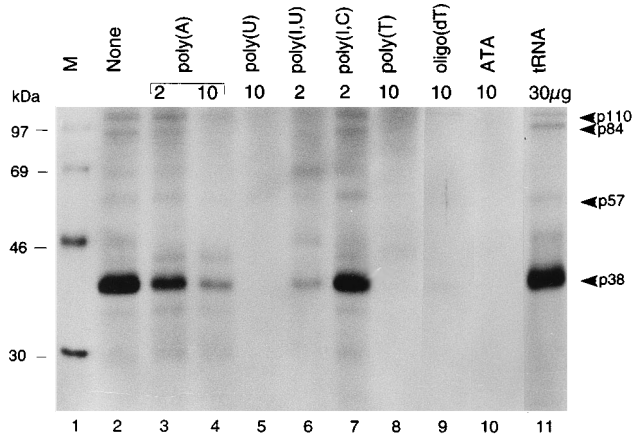

FIG. 7. Competition with specific and unspecific unlabeled polyribonucleotides and aurintricarboxylic acid (ATA). ^{33}P-labeled genomic-sense RNA502 was used for binding and label transfer to proteins present in the S-100 extract of HAV-infected MRC-5 cells. Concentrations are given in micrograms per reaction mixture (60 μl). The mobilities of marker proteins and the positions of cross-linked proteins are shown on the left and right sides, respectively.

because of their complementarity to the poly(A) tract. Poly(A) competed for label transfer from genomic-sense RNA502, but to a lesser extent (lanes 3 and 4). The label transfer from RNA502 to p38 in the presence of poly(I,C) was almost comparable to that of the control experiment, in which no competitor was added to the reaction mixture (lanes 2 and 7). Similar data were obtained with antigenomic RNA502 probe (data not shown). In this case, probably because of its complementarity to the poly(U) tract of antigenomic RNA502, poly(A) completely prevented label transfer to p38 when it was incubated in binding mixture prior to the addition of radioactive antisense RNA502. Poly(I,U), but not poly(I,C), competed well with antisense RNA502 (data not shown). tRNA of *E. coli* at a concentration of 0.5 mg/ml did not interfere with the specific binding of RNA502pos to proteins p38, p57, and p84 and was therefore used as a carrier, although to some extent it seemed to inhibit nonspecific interaction with high-molecular-weight proteins (lane 11).

When aurintricarboxylic acid, which is known to bind to the template site of DNA polymerase and RNA-dependent RNA polymerase (4, 19, 39), was added to the binding mixture at a concentration of 0.39 mM (Fig. 7, lane 10), the label transfer from RNA502 to p38 was completely abolished, indicating that aurintricarboxylic acid might bind to the same site within p38 as RNA502.

The 3′- and 5′-terminal HAV RNAs interact with the same cytoplasmic protein (p38). In preliminary experiments in which RNA representing the 5′-NTR of the HAV genome was used, it was apparent that p38 bound not only to the 3′ end but also to the 5′ terminus of the viral RNA. To test whether the 38-kDa protein bound to either end of the genome was identical, competition assays were performed. As shown in Fig. 8, genomic-sense RNA354 (first 354 bases of the HAV genome) as well as RNA502 (last 502 nt of the HAV genome) transferred the label to p38 present in the S-100 extract of mock-infected BS-C-1 cells; however, RNA354 bound to a lesser extent (lanes 3 and 4). In competition assays, a 50-fold molar excess of unlabeled RNA502 (3′ end) efficiently reduced label transfer to p38 from radioactive RNA354 and vice versa (lanes 1 and 6, respectively), strongly suggesting that p38 interacts with both the 5′ and the 3′ ends of the HAV genome.

DISCUSSION

Since it is of messenger sense, the picornavirus RNA serves two functions: translation and transcription. During the infec-

tion cycle, both processes must be regulated spatially as well as temporally so that the products of both processes, the HAV polyprotein and minus-strand RNA, respectively, are synthesized in appropriate amounts. Although it has been suggested that in vitro minus-strand synthesis of poliovirus is not dependent on cellular components and structures, it is reasonable to suppose that host proteins might assist in the recognition of the viral RNA in a manner similar to what has been observed for plus-strand RNA synthesis (for a review, see reference 38). Compared with other picornaviruses, HAV replicates at a greatly retarded rate without inducing a shutdown of host cell macromolecular synthesis. Several steps in the infection cycle have been proposed as rate-limiting factors in HAV amplification (1, 6, 13). One of these factors was ascribed to HAV RNA synthesis, which was considered to be down-regulated following the initial period of replicative activity (13). In an earlier report, we have shown that proteins found in persistently HAV-infected cells interact with nucleotide sequences of the 3′ end of the HAV genome (26). To understand the recognition signals initiating amplification of the HAV genome and in particular minus-strand RNA synthesis, we first analyzed the spectrum of cytoplasmic and ribosomal proteins which can interact with RNA probes representing different segments of the 3′ end of the HAV genome. In the initial experiments, we assessed the interaction of RNA502 with proteins present in mock- and HAV-infected cells, since this RNA, which represents not only the polyadenylated 3′-NTR but also preceding sequences encoding the C terminus of $3D^{pol}$, showed the strongest binding capacity. Among the ribosomal proteins that were cross-linked to RNA502 of both polarities, protein p52 was most abundant, in particular in mock-infected cells, when it was tested in initial experiments (Fig. 2, lanes 2 and 4). Because of the various binding extents of p52 and its considerable loss after HAV infection, we did not further study the ability of this protein to participate in RNA-protein interaction. In addition, cytoplasmic proteins with molecular masses of 38, 45, 57, 84, and 110 kDa were able to bind to RNA502. p57 was detected in HAV-infected cells in larger quantities and might therefore be one of the viral or cellular proteins induced as a result of HAV infection. Kinetic data favor the latter possibility, since the amount of this protein did not increase during the course of HAV infection (data not shown). Less label was transferred to p45, p57, p84, and p110, after UV cross-linking than to p38. However, the relative amounts of ^{33}P-label that were transferred to these proteins were similar for all four 3′-terminal RNAs tested. Proteins p38 and p57 have different ionic requirements for binding to RNAs, probably reflecting their environmental salt conditions in vivo. This observation is reminiscent of the finding by Chang et al. concerning cellular proteins p30 and p39 (10). Whether these proteins, in particular p38, are a part of the initiation complex leading to minus-strand RNA synthesis will have to be studied.

One intriguing observation was the finding that p38 recognized 3′ transcripts with different intensities. Since RNA90 and also RNA413 were less reactive with p38 and also competed less efficiently than longer RNA probes (Fig. 4 through 6), it is suggested that multiple interaction sites exist between the structural elements of the 3′-terminal RNA region and p38. The stem-loop structures formed by RNA90, which represents exactly the 3′-NTR–poly(A) domain, and by RNA413, which encodes the last 413 coding bases, seem to be sufficient but not optimal for interaction with p38. More-pronounced interaction with p38 was observed when these two RNAs were combined within one transcript (RNA502 and RNA1583). Although no direct biochemical data for the structure of the PK are available, the binding studies provide strong indirect evidence that additional higher-order structural elements are required for optimal interaction with p38 and other host proteins (Fig. 1B). This element (the PK) can be formed only when nt 7367 to 7433 are part of the RNA probe. PK elements have been first observed at the 3′ ends of several plant viruses which resume a tRNA-like structure (29). Biochemical and genetic evidence for a PK structure at the 3′ termini of the poliovirus and coxsackievirus genomes has been provided, and a correlation between this structure and its function in RNA amplification was established (20, 21). The PK proposed here for the 3′ terminus of the HAV genome is similar to that of coxsackievirus B1 in that it contains a stem-loop just upstream of the translational termination codon. Since RNA1583 enhanced neither interaction with p38 (Fig. 4) nor competition with shorter RNAs (Fig. 5 and 6) compared with RNA502, it may be assumed that putative higher-order structural elements located between nt 5917 and 6998 do not further contribute to the observed RNA-protein interaction. Interestingly, an RNA PK element was proposed to be formed also by the 5′-terminal sequences of the HAV genome (8, 9). In the light of our observation that p38 interacts with both the 5′- and the 3′-terminal sequences of the HAV genome (Fig. 8), it is tempting to speculate that the PK structure might be the prerequisite for specific interaction of p38 with viral RNA (see below). It would certainly be a fascinating feature of the virus replication strategy to employ the same host protein(s) for recognition of the RNA secondary structure formed by either terminus of the viral RNA.

To characterize further the RNA-protein interaction, the results of competition of various homo- and heteropolymeric polynucleotides as well as antisense probes with 3′ end transcripts were analyzed. The data shown here support our earlier observation that the specificity of the RNA-protein interaction is based on secondary structure rather than on the nucleotide sequence of the 3′-NTR or upstream regions. This is supported by the fact that antigenomic transcripts are recognized by cytoplasmic proteins equally well as genome-sense RNA, suggesting that they resume the same configuration. The fact that poly(U), poly(I,U), poly(T), and oligo(dT) competed much more efficiently than poly(A) may be due to the ability of these polymers to disrupt base pairing of the poly(A) tract and thus to prevent the formation of one of the stem-loop structures. The control experiments in which poly(A) inhibited the binding of antigenomic RNA give strong support to this conclusion. For the interaction of EMCV RNA polymerase 3D with the 3′-NTR, direct evidence was provided that the 3′-poly(A) is important for template selection and recognition (12).

Cellular tropism of picornaviruses and host range are dependent not only on the presence of a specific cell surface receptor but also on the cytoplasmic protein makeup, as was shown for poliovirus, which can replicate in mouse cells expressing the human poliovirus receptor (see reference 38). The current hypothesis favors the idea that specific intracellular factors and their interaction with viral components are of crucial importance for the efficiency of replication as well as translation of the picornavirus genome. One of the intracellular proteins essential for the recognition of viral RNA by 3D polymerase might be p38, which we detected in all mammalian cells tested thus far. In a recent study, a protein migrating with a similar mobility and able to bind to the 5′ end of poliovirus was identified as the N-terminal fragment of the eucaryotic elongation factor EF-1a, which is highly abundant in the cytoplasm (2, 3, 20). It will be interesting to find whether poliovirus and HAV utilize the same host protein for initiating viral RNA replication. RNA viruses of other families have selected dif-

ferent cytoplasmic proteins that probably assist in RNA replication. The 3′ end of the brome mosaic virus RNA was found to contribute to virus replication (23). For rubella virus, it was shown very recently that calreticulin, a phosphorylated calcium-binding protein, interacts with a stem-loop structure at the 3′ end of the viral RNA (35), whereas the 3′ end of Sindbis virus binds to 50- and 52-kDa proteins (27).

Similar to our finding that host proteins interact with the 3′-terminal RNA sequences of the HAV genome, it was shown that cell-type-specific proteins bound to various segments of the 5′-NTR of HAV RNA (10). One of these proteins migrated with a mobility similar to that of p38. This protein, which was detected in the RSW, bound very efficiently to the RNA probe that was used in our study. This finding probably reflects the bifunctional role of the IRES element in controlling not only internal initiation of translation but also viral RNA synthesis, as was recently shown for poliovirus (5, 31). In light of these data, it is not surprising that the 5′ and 3′ termini of the HAV genome could interact with the same cellular protein. Further studies are needed to prove whether this ribosome-associated and cell-type-specific protein is identical to the protein labeled by 3′-terminal probes. We are currently investigating the functional role of viral and cellular proteins in RNA amplification, in particular the interaction of these proteins with either terminus of the HAV genome.

ACKNOWLEDGMENTS

This work was supported by grants from the Schweizerischer Nationalfonds zur Förderung der wissenschaftlichen Forschung and in part from the Deutsche Forschungsgemeinschaft (DFG SFB 367 project B7).

We thank Stanley M. Lemon for providing BT7-H cells and plasmid pΔ355.

REFERENCES

1. **Anderson, D. A., and B. Ross.** 1990. Morphogenesis of hepatitis A virus: isolation and characterization of subviral particles. J. Virol. **64:**5284–5289.
2. **Andino, R., G. E. Rieckhof, P. L. Achacoso, and D. Baltimore.** 1993. Poliovirus RNA synthesis utilizes an RNP complex formed around the 5′-end of viral RNA. EMBO J. **12:**3587–3598.
3. **Andino, R., G. E. Rieckhof, and D. Baltimore.** 1990. A functional ribonucleoprotein complex forms around the 5′ end of poliovirus RNA. Cell **63:** 369–380.
4. **Blumenthal, T., and T. A. Landers.** 1973. The inhibition of nucleic acid-binding proteins by aurintricarboxylic acid. Biochem. Biophys. Res. Commun. **55:**680–688.
5. **Borman, A. M., F. G. Deliat, and K. M. Kean.** 1994. Sequences within the poliovirus internal ribosome entry segment control viral RNA synthesis. EMBO J. **13:**3149–3157.
6. **Borovec, S. V., and D. A. Anderson.** 1993. Synthesis and assembly of hepatitis A virus-specific proteins in BS-C-1 cells. J. Virol. **67:**3095–3102.
7. **Brantly, J. D., and A. G. Hund.** 1993. The N-terminal protein of the polyprotein encoded by potyvirus tobacco vein mottling virus is an RNA-binding protein. J. Gen. Virol. **74:**1157–1162.
8. **Brown, E. A., S. P. Day, R. W. Jansen, and S. M. Lemon.** 1991. The 5′ nontranslated region of hepatitis A virus RNA: secondary structure and elements required for translation in vitro. J. Virol. **65:**5828–5838.
9. **Brown, E. A., A. J. Zajac, and S. M. Lemon.** 1994. In vitro characterization of an internal ribosomal entry site (IRES) present within the 5′ nontranslated region of hepatitis A virus RNA: comparison with the IRES of encephalomyocarditis virus. J. Virol. **68:**1066–1074.
10. **Chang, K. H., E. A. Brown, and S. M. Lemon.** 1993. Cell type-specific proteins which interact with the 5′ nontranslated region of hepatitis A virus RNA. J. Virol. **67:**6716–6725.
11. **Cohen, J. I., J. R. Ticehurst, S. M. Feinstone, B. Rosenblum, and R. H. Purcell.** 1987. Hepatitis A virus cDNA and its RNA transcripts are infectious in cell culture. J. Virol. **61:**3035–3039.
12. **Cui, T., S. Sankar, and A. Porter.** 1993. Binding of encephalomyocarditis virus RNA polymerase to the 3′-noncoding region of the viral RNA is specific and requires the 3′-poly(A) tail. J. Biol. Chem. **268:**26093–26098.
13. **deChastonay, J., and G. Siegl.** 1987. Replicative events in hepatitis A virus-infected MRC-5 cells. Virology **157:**268–275.
14. **Dildine, S. L., and B. L. Semler.** 1992. Conservation of RNA-protein interactions among picornaviruses. J. Virol. **66:**4364–4376.
15. **Flanegan, J. B., and T. A. van Dyke.** 1979. Isolation of soluble and template-dependent poliovirus RNA polymerase that copies virion RNA in vitro. J. Virol. **32:**155–161.
16. **Francki, R. I. B., C. M. Fauquet, D. L. Knudson, and F. Brown.** 1991. Classification and nomenclature of viruses. Arch. Virol. **2:**320–326.
17. **Freier, S. M., R. Kierzek, J. A. Jaeger, N. Sugimoto, M. H. Caruthers, T. Neilson, and D. H. Turner.** 1986. Improved free-energy parameters for predictions of RNA duplex stability. Proc. Natl. Acad. Sci. USA **83:**9373–9377.
18. **Giachetti, C., S.-S. Hwang, and B. L. Semler.** 1992. *cis*-acting lesions targeted to the hydrophobic domain of a poliovirus membrane protein involved in RNA replication. J. Virol. **66:**6045–6057.
19. **Givens, J. F., and K. F. Manly.** 1976. Inhibition of RNA-directed DNA polymerase by aurintricarboxylic acid. Nucleic Acids Res. **3:**405–418.
20. **Harris, K. S., W. Xiang, L. Alexander, W. S. Lane, A. V. Paul, and E. Wimmer.** 1994. Interaction of poliovirus polypeptide $3CD^{pro}$ with the 5′ and 3′ termini of the poliovirus genome. J. Biol. Chem. **269:**27004–27014.
21. **Jacobson, S. J., D. A. M. Konings, and P. Sarnow.** 1993. Biochemical and genetic evidence for a pseudoknot structure at the 3′ terminus of the poliovirus RNA genome and its role in viral RNA amplification. J. Virol. **67:** 2961–2971.
22. **Jaeger, J. A., D. H. Turner, and M. Zuker.** 1989. Improved prediction of secondary structures for RNA. Proc. Natl. Acad. Sci. USA **86:**7706–7710.
23. **Lahser, F. C., L. E. Marsh, and T. C. Hall.** 1993. Contribution of the brome mosaic virus RNA-3 3′-nontranslated region to replication and translation. J. Virol. **67:**3295–3303.
24. **Lama, J., A. V. Paul, K. S. Harris, and E. Wimmer.** 1994. Properties of purified recombinant poliovirus protein 3AB as substrate for viral proteinases and as co-factor for RNA polymerase $3D^{pol}$. J. Biol. Chem. **269:**66–70.
25. **Le, S.-Y., J.-H. Chen, N. Sonnenberg, and J. V. Maizel.** 1993. Conserved tertiary structural elements in the 5′ nontranslated region of cardiovirus, aphthovirus and hepatitis A virus RNAs. Nucleic Acids Res. **21:**2445–2451.
26. **Nuesch, J., M. Weitz, and G. Siegl.** 1993. Proteins specifically binding to the 3′ untranslated region of hepatitis A virus RNA in persistently infected cells. Arch. Virol. **128:**65–79.
27. **Pardigon, N., E. Lenches, and J. H. Strauss.** 1993. Multiple binding sites for cellular proteins in the 3′ end of Sindbis alphavirus minus-sense RNA. J. Virol. **67:**5003–5011.
28. **Pilipenko, E. V., S. V. Maslova, A. N. Synyakov, and V. Agol.** 1992. Towards identification of *cis*-acting elements involved in the replication of enterovirus and rhinovirus RNAs: a proposal for the existence of tRNA-like terminal structures. Nucleic Acids Res. **20:**1739–1745.
29. **Pleij, C. W. A.** 1990. Pseudoknots: a new motif in the RNA game. Trends Biochem. Sci. **15:**143–147.
30. **Porter, A. G.** 1993. Picornavirus nonstructural proteins: emerging roles in virus replication and inhibition of host cell functions. J. Virol. **67:**6917–6921.
31. **Rohll, B. J., N. Percy, R. Ley, D. J. Evans, J. W. Almond, and W. S. Barclay.** 1994. The 5′-untranslated regions of picornavirus RNAs contain independent functional domains essential for RNA replication and translation. J. Virol. **68:**4384–4391.
32. **Sambrook, J., E. F. Fritsch, and T. Maniatis.** 1989. Molecular cloning: a laboratory manual, 2nd ed. Cold Spring Harbor Laboratory, Cold Spring Harbor, N.Y.
33. **Schultheiss, T., Y. Y. Kusov, and V. Gauss-Müller.** 1994. Proteinase 3C of hepatitis A virus (HAV) cleaves the HAV polyprotein P2-P3 at all sites including VP1/2A and 2A/2B. Virology **198:**275–281.
34. **Siegl, G.** 1992. Replication of hepatitis A virus and processing of proteins. Vaccine **10:**32–35.
35. **Singh, N. K., C. D. Atreya, and H. L. Nakhasi.** 1994. Identification of calreticulin as a rubella virus RNA binding protein. Proc. Natl. Acad. Sci. USA **91:**12770–12774.
36. **Weitz, M., and G. Siegl.** 1993. Hepatitis A virus: structure and molecular virology, p. 21–34. *In* A. J. Zuckermann and H. C. Thomas (ed.), Viral hepatitis, Scientific Basis and Clinical Management. Churchill Livingstone Publishing Co., London.
37. **Whetter, L. E., S. P. Day, O. Elroy-Stein, E. A. Brown, and S. M. Lemon.** 1994. Low efficiency of the 5′ nontranslated region of hepatitis A virus RNA in directing cap-independent translation in permissive monkey kidney cells. J. Virol. **68:**5253–5263.
38. **Wimmer, E., C. U. T. Hellen, and X. Cao.** 1993. Genetics of poliovirus. Annu. Rev. Genet. **27:**353–436.
39. **Zabel, P., I. Jongen-Neven, and A. van Kammen.** 1979. In vitro replication of cowpea mosaic virus RNA. III. Template recognition by cowpea mosaic virus RNA replicase. J. Virol. **29:**21–33.